Urban Climate 46 (2022) 101282

Contents lists available at ScienceDirect

Urban Climate

journal homepage: www.elsevier.com/locate/uclim

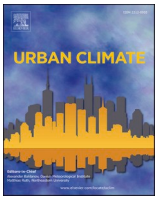

Measurement of recreational N_2O emissions from an urban environment in Manchester, UK

Patrick A. Barker [a,*], Grant Allen [a], Michael Flynn [a], Stuart Riddick [b], Joseph R. Pitt [c]

[a] School of Earth and Environmental Sciences, University of Manchester, Manchester M13 9PL, UK
[b] The Energy Institute, Colorado State University, 430 N. College Avenue, Fort Collins, CO 80523, USA
[c] School of Chemistry, University of Bristol, Cantock's Close, Bristol BS8 1TS, UK

ARTICLE INFO

Keywords:
Nitrous oxide
Greenhouse gas
Recreational N2O
UK

ABSTRACT

Nitrous oxide (N_2O) is a potent greenhouse gas that is currently the third largest contributor to anthropogenic radiative forcing. It is also a strong ozone depleting substance. Given this importance, mitigation of N_2O emissions remains important and sources must be understood in greater detail. In this study, in situ measurements of N_2O alongside a variety of other trace gases and aerosols were made from a ground-based air quality observation site in an urban environment of Fallowfield, Manchester, United Kingdom over a period of 12 months between October 2020 and October 2021. N_2O mole fraction was observed to be poorly correlated with other atmospheric pollutant tracers during the measurement period, with little evidence of co-enhancement (and therefore common source relationships) between N_2O and other local pollutant trace gases and aerosol. Large N_2O enhancements ($>$ 400 ppb above background) over short time scales ($<$ 2 min) were seen with no co-enhancement of other trace gases and aerosol concentrations, suggesting discrete N_2O sources in the near vicinity of the measurement site. Measured N_2O concentrations showed a consistent temporal pattern over day, week, and year timescales with consistently large weekend enhancements observed between the hours of 18:00 and 02:00 local time, suggesting the source of N_2O may be associated with night-time recreational use by nearby residents. These weekend-night-time temporal patterns were not correlated with other trace gases measured at the same location. Analysis of the air transport history of N_2O measurements showed high mean nocturnal mole fractions originating from the west and south-west of the observation site, suggesting that emissions may have originated from nearby areas of student accommodation and dense areas of private housing to the west. This study finds evidence for a detectable recreational N_2O source that appears to be dominant over other potential N_2O sources for the area studied. Further study is needed to quantify the local and national emission rates of this potentially increasing atmospheric pollution source, and to compare the magnitude of this source to other locations within the UK. The study demonstrates an important need to assess and validate National Atmospheric Emission Inventory (NAEI) estimates for recreational N_2O emissions.

1. Introduction

Nitrous oxide (N_2O) is a potent greenhouse gas with a global warming potential 298 times that of carbon dioxide, and the third most

* Corresponding author at: National Physical Laboratory, Hampton Road, Teddington, Middlesex TW11 0LW, UK.
E-mail address: pat.barker@npl.co.uk (P.A. Barker).

https://doi.org/10.1016/j.uclim.2022.101282
Received 7 March 2022; Received in revised form 16 July 2022; Accepted 1 September 2022
Available online 18 September 2022

important greenhouse gas in terms of contribution to anthropogenic climate change (IPCC, 2013). In addition, N_2O is the dominant stratospheric ozone depleting substance emitted in the 21st Century (Ravishankara et al., 2009). N_2O persists in the atmosphere for 114 ± 9 years (Prather et al., 2015), meaning that the impact of current emissions on climate and ozone will persist for many years to come. Mitigation of N_2O emissions can therefore benefit both climate impact and stratospheric ozone depletion. The global average mole fraction of N_2O in the troposphere has increased from a pre-industrial level of ~270 ppb to a current abundance of 334 ppb as of July 2021 (NOAA, 2021). Atmospheric growth of N_2O mole fraction persists at an estimated rate of 2% per decade, with post-industrial growth understood to be driven by anthropogenic activity, most significantly from the widespread use of fertilisers in agriculture (Tian et al., 2020).

Gaseous N_2O is frequently used as an anaesthetic during childbirth and in dentistry. However, it has also been used as a recreational substance throughout history due to its euphoria-inducing side effects (Zuck et al., 2012), with dangerous (and sometimes deadly) health implications (Randhawa and Bodenham, 2016). N_2O gas is typically inhaled when used recreationally from balloons filled from pressurised stainless-steel canisters designed for use in the food industry (shown in Fig. 1). Recreational use of N_2O in the UK is widespread (Ehirim et al., 2018; UK Home Office, 2018) and increasing (Randhawa and Bodenham, 2016). An estimated 7.6% of 16 to 24-year-olds in the UK reported recreational N_2O use in 2014 (Randhawa and Bodenham, 2016), which increased to 8.8% in 2018 (UK Home Office, 2018). Even though the physical risks, including dizziness, asphyxiation, and vitamin B12 deficiency, and environmental concerns regarding the casual disposal (littering) of the stainless-steel canisters have been reported, there is little public awareness of the additional environmental threat of N_2O emissions as a greenhouse gas or ozone-depleting substance. As there is no metabolization of N_2O in the body (Banks and Hardman, 2005), N_2O breathed in is exhaled to the atmosphere. The UK National Atmospheric Emission Inventory (NAEI) estimates an emission of 13 t of N_2O via recreational use in 2019, representing ~0.02% of the total UK N_2O budget for 2019 (75 Kt) (NAEI/BEIS, 2022). Despite the relatively small estimated contribution of recreational N_2O to the total source, there has been no measurement work to validate the NAEI estimate for recreational N_2O. In situ measurement studies of this source are therefore crucial for assessing the accuracy of inventory-reported recreational N_2O emissions.

There has hitherto been little research on N_2O emission sources from urban areas, and no known measurement-led study of detectable emissions from recreational use. Many studies have focused on soil N_2O emission from fertilised urban lawns and turf grasses (Townsend-Small and Czimczik, 2010; Van Delden et al., 2016), or riverine N_2O emissions from sewage input into urban river systems or from sewage treatment plants (Tallec et al., 2008; De Mello et al., 2013; Yu et al., 2013). Eddy covariance flux measurements of N_2O were reported for an urban environment in Edinburgh, UK by Famulari et al. (2010), in which a mean net flux of 91 ng $m^{-2}\,s^{-1}$ was measured, and a diurnal pattern indicated traffic N_2O emissions were a major source. A similar eddy covariance study was carried out in an urban area of Helsinki, Finland by Järvi et al. (2014), where a median N_2O flux of 21 ng $m^{-2}\,s^{-1}$ was measured. Significant fluxes were measured from traffic and from urban green areas, but the urban soils appeared to be the largest N_2O emission sources in the Järvi et al. (2014) study. In summary, there are limited examples of urban N_2O emission studies where direct fluxes have been derived, and there has yet to be any in situ measurement studies investigating the presence and extent of N_2O emission from recreational sources.

This paper presents results from continuous in situ N_2O mole fraction measurements from a ground-based observation site in an urban environment. Measurements were made over a period of 12 months between October 2020 and October 2021 from an air quality measurement site in Fallowfield, Manchester operated by the University of Manchester. In the following sections, a statistical climatology of the measurements over the year-long period is described in conjunction with spatial and temporal trends, where N_2O mole fractions demonstrate weak correlations with other atmospheric pollutant tracers that would otherwise suggest co-emission from sources other than recreational use. Finally, the presence of a potential recreational source in the vicinity of the site based on diurnal mole fraction variability and weekend overnight maxima are discussed.

Fig. 1. Photograph of discarded nitrous oxide whipped cream charger canisters in Manchester, UK. Nitrous oxide from these canisters is used to fill balloons, from which the gas is then inhaled for short-term euphoric effect.

2. Materials and methods

2.1. Site description

Measurements of typical urban pollutant trace gases, aerosols, and meteorological parameters (see Table 1) were made at the Manchester Air Quality Supersite (MAQS) (53° 26′ 39.20"N, 2° 12′ 52.20"W) situated in the University of Manchester Fallowfield campus, approximately four kilometres south of Manchester city centre. Fig. 2 shows the location of the MAQS and the surrounding Fallowfield area. Two single-carriage British A-class roads pass along the south and west of the measurement site, with a high density of shops, bars and restaurants situated to the southwest. Student accommodation buildings surround the site from the south to north-east in a clockwise direction. Three car parks are also situated to the north, east, and south-east of the measurement site.

2.2. Instrumentation

The MAQS is comprised of a stack of four shipping containers housing an array of in situ trace gas and aerosol instrumentation, a picture of the MAQS site is shown in Fig. 3. All enclosures are mains-powered and air-conditioned. Inlets for all instruments and meteorological instrumentation are situated on the top of the shipping container stack at a height of 7 m above ground level. Continuous measurement of N_2O mole fraction started at 13:30 UTC on 28 October 2020 and remains ongoing at the time of writing (reported up to 19 October 2021 in this study). Concurrent measurements of CH_4, CO_2, CO, O_3, NO, NO_2, $PM_{2.5}$, PM_{10}, and meteorological parameters were recorded throughout the same period. All data were averaged to a 1-minute sampling frequency for analysis in this work. The parameters used in this work, along with their instruments, operational ranges and precisions, and sampling frequencies are displayed in Table 1.

N_2O dry-air mole fractions were measured using an Aerodyne Quantum Cascade Laser Absorption Spectrum (QCLAS), described by Pitt et al. (2016). The QCLAS instrument uses a single thermoelectrically cooled quantum cascade laser tuned to a wavelength of ~4.5 μm and calibrated using three calibration gas standards, all of which are traceable to the World Meteorological Organisation (WMO) X2006A calibration scale for N_2O. A 1σ precision of 0.3 ppb was calculated for 1 Hz N_2O mole fraction measurements during the measurement period. Mole fractions of CH_4 and CO_2 were measured using a Los Gatos Research (LGR) Multi-gas Carbon Emissions Analyser, which utilises the off-axis Integrated Cavity Output Spectroscopy (OA-ICOS) technique. The LGR instrument had a precision of 0.3 ppm for CO_2 and 2 ppb for 1 Hz CH_4 measurements. Mole fractions of CO were measured with a Thermo Scientific Model 48i Infrared CO Analyser, with an uncertainty of 0.1 ppb at 20 s sampling frequency. Mole fractions of NO were measured using a Thermo Scientific Model 42i-y Chemiluminescence NO_y Analyser, which has an uncertainty of 0.4 ppb at 20 s sampling rate. NO_2 was measured using a Teledyne API T500U Cavity Attenuated Phase Shift (CAPS) Analyser, with an uncertainty of 10% at 10 s measurement frequency. Particulate matter ($PM_{2.5}$ and PM_{10}) concentrations in ug m^{-3} were measured at 1 min sampling frequency using a Palas Fidas 200 S Aerosol Spectrometer, with a $< 10\%$ uncertainty on these measurements. Measurements of wind speed and direction were acquired using a Gill Windmaster Sonic Anemometer, with a precision of 0.01 m s^{-1} for wind speed and 0.1° for wind direction.

3. Results and discussion

This section will discuss the spatial and temporal trends in N_2O and other trace-gas concentrations over the 12-month measurement period to assess source behaviour and location. Section 3 will first discuss the correlation of N_2O mole fraction with other atmospheric tracers to understand potential sources of co-emission. Following this, the temporal variability of N_2O and other trace gases over an average day, week, and over the course of the year will be discussed to determine likely source behaviour based on temporal enhancement patterns. In addition to temporal analysis, qualitative spatial analysis of trace gas variability with wind speed and direction will also be described, including a brief overview of the climatology during the measurement period followed by an analysis of trace gas enhancement as with wind direction.

Table 1
Trace gases, aerosols, and meteorological parameters measured at the MAQS that feature in this work, the instruments models, instrumental ranges and precisions, and measurement frequencies are also shown.

Species/Parameter	Instrument	Range and Precision	Sampling Frequency
Ozone (O_3)	Thermo 49i	0.5 ppb – 200 ppm, 1 ppb	20 s
Nitric Oxide (NO)	Thermo 42i-y	50 ppt – 1000 ppb, 0.4 ppb	20 s
Nitrogen Dioxide (NO_2)	Teledyne API T500U (CAPS)	40 ppt – 1000 ppb, 0.5%	10 s
Carbon Monoxide (CO)	Thermo 48i	0.04–10,000 ppm, 0.1 ppm	20 s
Carbon Dioxide (CO_2)	LGR Multi-gas Carbon Emissions Analyser	0.1–3000 ppm, 0.3 ppm	1 s
Methane (CH_4)	LGR Multi-gas Carbon Emissions Analyser	0.3 ppb – 100 ppm, 2 ppb	1 s
Nitrous Oxide (N_2O)	Aerodyne QCLAS	Precision: 0.58 ppb	1 s
Particulate Matter ($PM_{2.5}$, PM_{10})	Palas FIDAS200	0–10,000 μg m^{-3}, < 10%	1 min
Wind Speed and Direction	Gill Windmaster Sonic Anemometer	0–50 m s^{-1}, 0.01 m s^{-1} 0–359°, 0.1°	20 Hz
Temperature and Pressure		T: −40 - +60 °C P: 500–1100 hPa	1 min

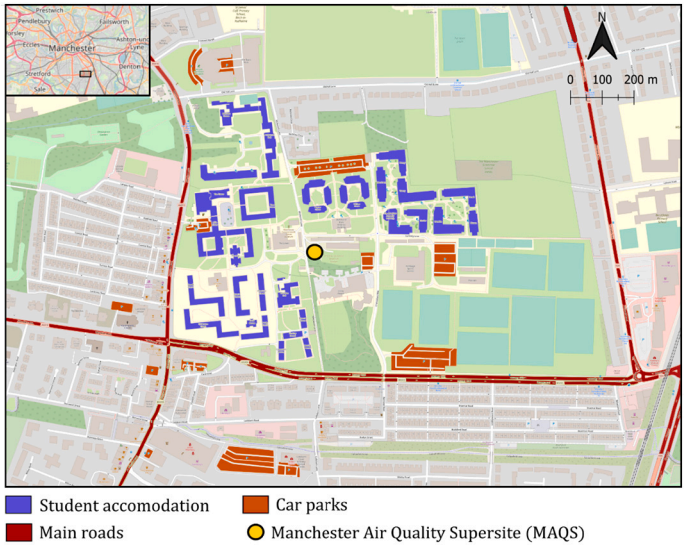

Fig. 2. Map of the area surrounding the MAQS (shown as a yellow circle). Student accomodation buildings are highlighted in blue, main roads are shown in red, and car parking areas are shown in orange. (For interpretation of the references to colour in this figure legend, the reader is referred to the web version of this article.)

Fig. 3. Photograph of the MAQS. Trace gas and aerosol instruments are enclosed within the shipping containers. Instrument inlets, pressure and temperature sensors, and the sonic anemometer are situated on top of the container stack.

3.1. N_2O-tracer relationships

Fig. 4 shows a time series of measured pollutant trace gas and aerosol concentrations across the measurement period. Small gaps in the N_2O dataset (e.g. early Jan 2021) were due to unscheduled power losses and technical issues. Fig. 4 shows evidence of co-emission between some of the trace gases measured at the site, most notably CH_4, CO_2, CO, NO_x and, to some extent, particulate matter. Emission of these species and the correlation between them is expected to be associated with vehicles from nearby roads (Ketzel et al., 2003), whereas the large enhancements in particulate matter accompanied by more modest enhancements in NO_x, CO, and greenhouse gases are likely the result of biomass burning (Andreae, 2019). Of particular note is the potential relationship with the use of fireworks

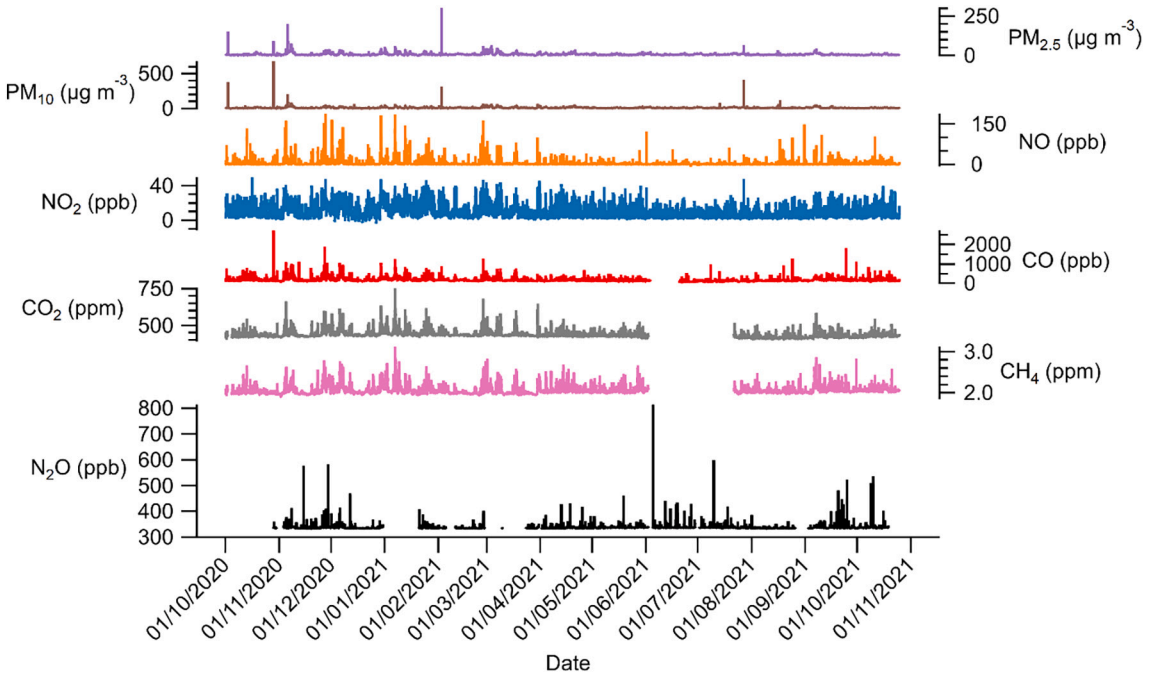

Fig. 4. One-minute-average time series of concentrations of $PM_{2.5}$, PM_{10}, NO, NO_2, CO, CO_2, CH_4, and N_2O from the MAQS from October 2020 to October 2021.

as a number of the large particulate matter enhancements occur close to Guy Fawkes Night (05 November 2021), when fireworks and urban outdoor fires are common in the UK (Vecchi et al., 2008). Contrary to typical urban source relationships between air quality tracers (such as those indicative of traffic emissions), N_2O does not display the same common pattern of enhancement with other trace gas and aerosol species.

The common emission patterns observed between tracers are also illustrated by the correlation matrix in Fig. 5. Relatively high correlation coefficients (> 0.5) were observed between CH_4, CO_2, CO, and NO_x, which all showed common patterns of enhancement seen in the time series in Fig. 4. High correlation between relatively well-mixed and unreactive trace gases such as CO_2 and CH_4 is likely influenced by diurnal mole fraction variation with boundary layer dynamics over the day/night. Vertical turbulent motion during the daytime mixes pollution into background air more effectively, resulting in lower mean mole fractions during daylight hours.

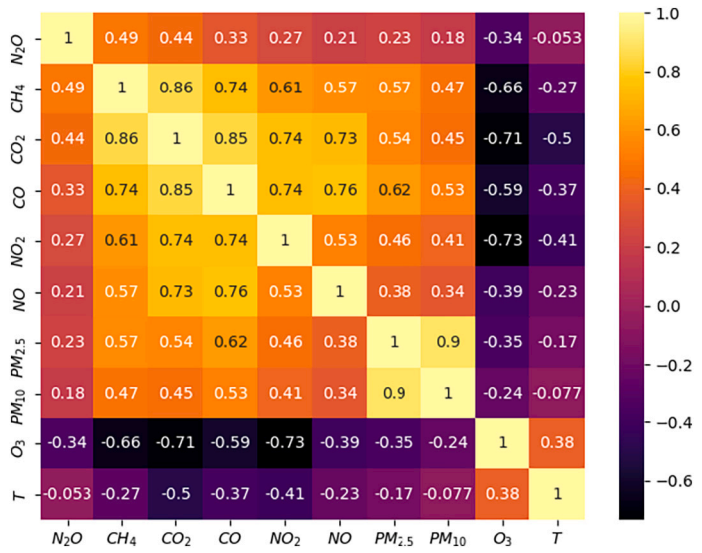

Fig. 5. Correlation matrix for various trace gases, aerosols and temperature measured at the MAQS between October 2020 and October 2021. Pearson correlation coefficients of the various species/parameters are shown in the boxes, and boxes are coloured by correlation coefficient.

In contrast, the nocturnal boundary layer is typically more stable, trapping urban surface emissions and resulting in higher average nocturnal mole fractions. N_2O is notably less well correlated with all other trace gases, with correlation coefficients consistently lower than 0.5. Of all species, N_2O mole fraction has the highest positive correlation with CH_4 and CO_2 mole fractions, with coefficients of 0.49 and 0.44 respectively.

Fig. 6 shows scatter plots of selected species and temperature versus N_2O mole fraction. It can be seen that there were modest enhancements of N_2O (approximate 10–20 ppb above background) that coincided with high enhancements of NO_x, CO, CO_2 and CH_4. However, very high N_2O enhancements (up to 400 ppb above background) do not appear to be correlated with enhancements of any other species measured at the MAQS site, as shown by the horizontal linear enhancements shown in Fig. 6. Rather, all of the aforementioned large N_2O enhancements appear to be relatively sudden increases in mole fraction that were only observed on timescales of a few minutes. The sudden onset and transient nature of N_2O enhancement (relatve to other gases) suggests that the source of these N_2O emissions was in relatively close proximity to the measurement site rather than originating from longer range transport of a more well-mixed airmass.

In summary, there appears to be weak correlation between N_2O and other trace gas and aerosol species, especially at lower N_2O concentrations (< 50 ppb over background), which we expect to be a result of co-emission from traffic, biomass burning, and other typical urban emission sources. Much larger enhancements in N_2O (50–400 ppb over background) were observed with no correlation to any other measured tracers, suggesting the presence of a significant nearby source of solely N_2O that does not appear to originate from other urban emission sources such as traffic or combustion.

3.2. Temporal variability

The temporal trends in trace gas observations are used here to understand emission source behaviour and to identify the dominant emission sources in the area.

3.2.1. Time of day

Fig. 7 shows the statistical variability of N_2O, CH_4, CO and NO over daily, weekly, and yearly timescales, with variability over the span of a day shown on the left panels. Solid lines show the median concentrations, darker shaded regions show the 25th to 75th percentile range, and the lighter shaded areas show the 5th to 95th percentile range. N_2O exhibits a diurnal pattern of enhanced nocturnal mole fraction relative to daytime concentrations, with mole fractions increasing from ~18:00 onwards, peaking at approximately 02:00 before declining rapidly thereafter. The most prevalent use of recreational N_2O is known to occur at house parties (van Amsterdam et al., 2015). Such events most often occur from evening to early morning, which coincides with the nocturnal period of enhanced N_2O shown in Fig. 7. It is therefore a strong possibility that the evening to early morning N_2O enhancements observed here

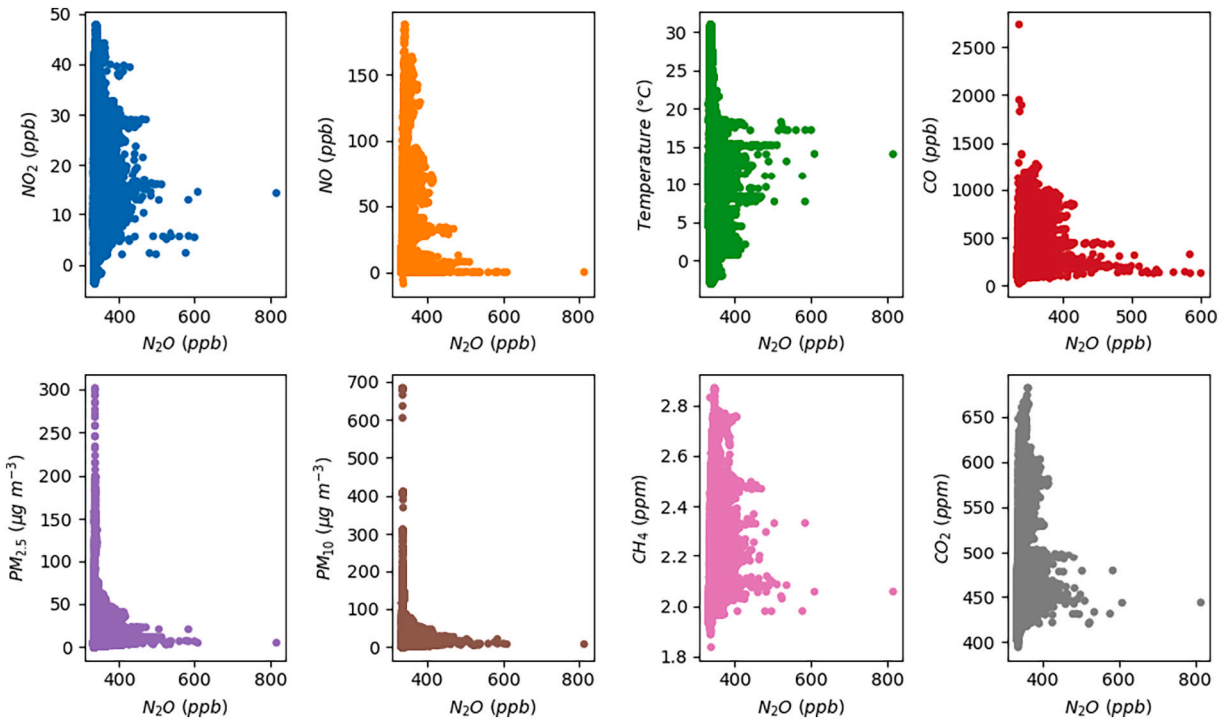

Fig. 6. Scatter plots of NO_2, NO, CO, CH_4, CO_2, $PM_{2.5}$, PM_{10}, and temperature versus N_2O for October 2020 – October 2021 measurements at the MAQS.

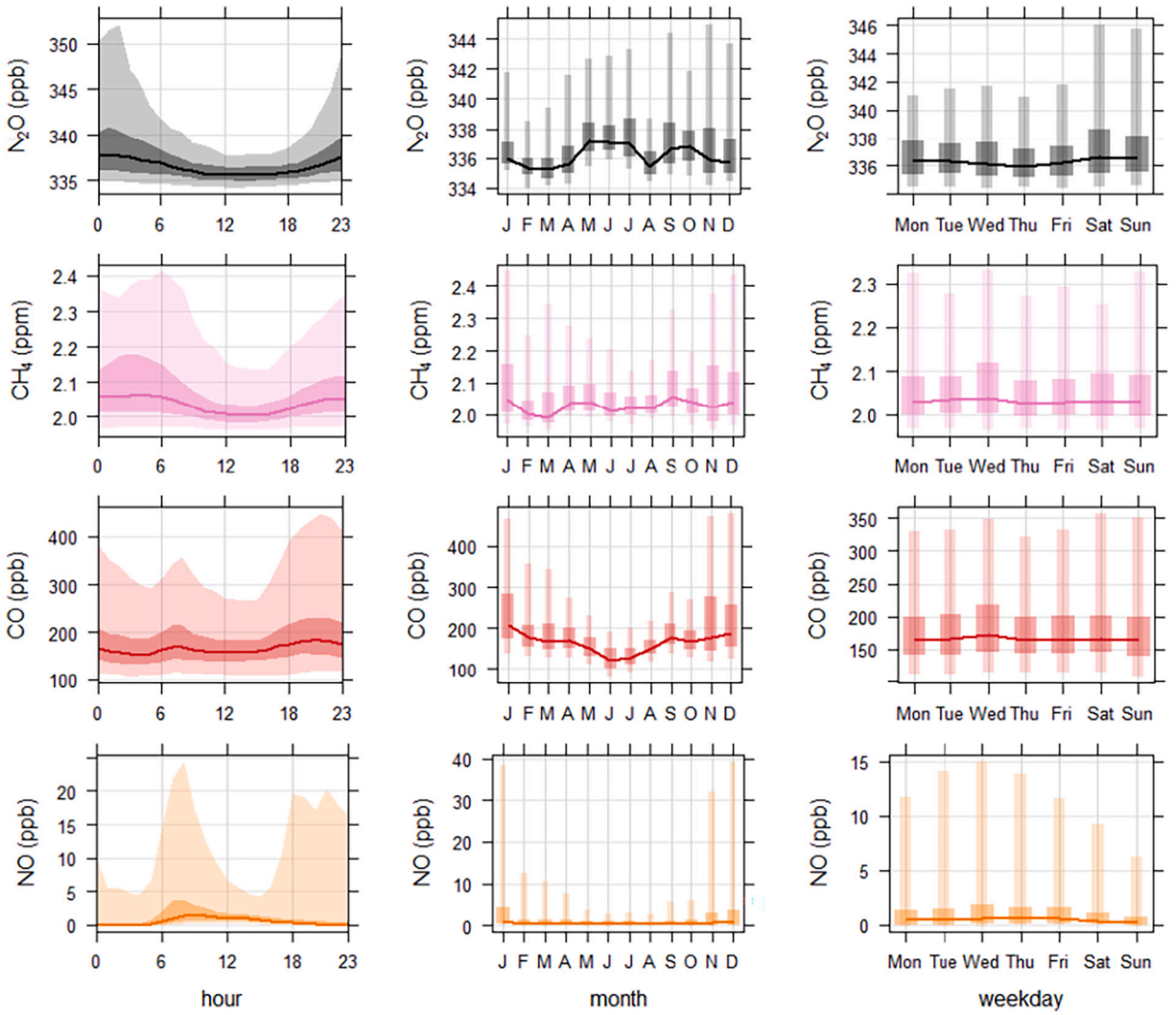

Fig. 7. N_2O, CH_4, CO, and NO mole fraction variability with hour of the day (left), month of the year (middle), and day of the week (right). Solid lines represent median values, darker shaded areas represent the 25th to 75th percentile range, and lighter shaded areas represent the range between the 5th and 95th percentiles.

primarily result from recreational N_2O use.

As with N_2O, CH_4 displays a diurnal enhancement pattern, with a 95th percentile maximum between approximately 21:00 and 06:00, before declining thereafter to a minimum between 12:00 and 17:00. There are a lack of significant CH_4 point sources within close proximity of the site that follow a nocturnal pattern of emission seen in Fig. 7; traffic CH_4 emissions would be minimal, and would show likely exhibit morning-afternoon commuter traffic spikes (Squires et al., 2020), large-scale gas leaks may represent a significant source, but are likely transient in nature, and would not persist throughout the measurement period. It is therefore likely that CH_4 mole fraction is well mixed at the MAQS. As a result of the well-mixed nature of CH_4 here, the nocturnal enhancements are consistent with ventilation and dilution as a result of boundary layer dynamics (Davies et al., 2007). Pooling of local emissions (i.e. from small leaks in domestic gas infrastructure or from wastewater treatment) at night and subsequent reduction in mole fraction with boundary layer development (mixing and ventilation) in daylight hours (Helfter et al., 2016; Daelman et al., 2012). Despite the presence of diurnal patterns in both N_2O and CH_4, there appear to be notable differences between the time profiles of both gases. Firstly, N_2O enhancement peaks earlier in the morning than CH_4; N_2O decreases sharply after 02:00 whereas CH_4 remains enhanced until 06:00 before the mole fraction begins to decrease. Furthermore, the nocturnal N_2O enhancement is sustained for a far shorter time than with CH_4, with a rapid increase to peak enhanced N_2O at 02:00 followed by a sharp decline as opposed to relatively constant enhanced CH_4 between 23:00 and 16:00. The difference between the diurnal profiles of N_2O and CH_4 suggests that while daily CH_4 mole fraction variability is governed largely by boundary layer dynamics, N_2O variability is additionally influenced by a combination of boundary layer dynamics and a strong nearby recreational N_2O source as evidenced by the difference in temporal profile with CH_4.

As opposed to the diurnal profiles of N_2O and CH_4, NO and CO both exhibit a similar daily trend of morning enhancement peaking

at approximately 07:00, followed by an afternoon enhancement from approximately 17:00 onwards. This morning-afternoon trend is consistent with emissions from commuter traffic. There is some evidence of the same boundary layer driven diurnal profile seen in CH_4 present in CO, but not in NO. NO does not exhibit the same diurnal pattern associated with boundary layer dynamics as seen in longer-lived species such as CH_4 and CO, due to its short lifetime (on the order of hours depending on solar radiation, temperature, and O_3 abundance (Larin and Kuskov, 2014; Kenagy et al., 2018)). The absence of a commuter traffic source pattern in the temporal profile of N_2O suggests that traffic is not a dominant N_2O source in this region, hence nocturnal recreational N_2O emissions may be significantly higher than N_2O from a vehicular source in this area.

3.2.2. Day of week

The right-hand panels of Fig. 7 shows the variability in trace gas mole fraction over a weekly timescale. It can be seen that N_2O mole fraction is relatively constant during weekdays, but significantly enhanced on Saturdays and Sundays. The 95th percentile N_2O mole fraction is in the range of 341–342 ppb from Monday to Friday but increases by ~4 ppb to 345–346 ppb during the weekend. Fig. 8 shows the variability in mean N_2O mole fraction over the course of a day, but is coloured by day of the week in order to further illustrate changes observed at the weekend. It can be seen that there are two clear modes of N_2O mole fraction variability for weekends and weekdays which appear to only deviate from each other between 20:00 and 06:00. Interestingly, Friday evenings are similar to weekend mode of N_2O enhancement, whereas Sunday evenings do not follow this weekend pattern, instead more closely resembling the typical weekday mode. The specific times during the weekend (approximately 20:00 to 06:00 from Fig. 8) that N_2O is enhanced relative to weekdays suggest that the source of the nocturnal N_2O enhancements could be from the use of N_2O as a recreational substance. In contrast to N_2O, NO mole fraction is lower on weekend days with a minimum on Sundays due to commuter traffic being the dominant NO_x source in the area. Additionally, there appears to be little sensitivity of CH_4 or CO mole fraction to the day of week, with median values and interquartile ranges remaining relatively consistent between days of the week. The lack of weekend sensitivity in CH_4 and CO is consistent with the boundary layer influence on their mole fractions identified in Section 3.2.1, as this behaviour would be constant throughout the week. None of the other species share the pattern of weekend enhancement seen in N_2O mole fraction, suggesting that the source of N_2O responsible for these enhancements is discrete, with no co-emission of other tracers.

3.2.3. Time of year

The variability of trace gas mole fraction over the course of the year-long measurement period is shown in the central column of Fig. 7. There appears to be little seasonal sensitivity in N_2O mole fraction in contrast to other trace gases, with minima in median, 75th, and 95th percentile N_2O mole fraction in February, March, and August. The lower February and March mole fractions are potentially a result of the significant gaps in N_2O data acquisition during these months due to unplanned instrument shutdowns. N_2O mole fraction appears to rapidly decrease from July to August, but recovers to a similar magnitude in September. This sharp August drop could be the result of the summer university break from 11 June 2021 to 20 September 2021. There is likely a lower number of students occupying nearby accommodation buildings in August, resulting in a reduced recreational N_2O source from these buildings during this time.

As opposed to N_2O, CO and NO mole fractions display a more predictable seasonal variability that can be explained by changing meteorological conditions. Both CO and NO show lower mole fraction enhancement over summer months than winter, with NO and CO minima occurring in July and maxima in December. This is to be expected from the vertical convection of surface emissions in warmer summer months, resulting in better air quality. There is evidence of the same yearly pattern in CH_4 mole fraction shown by the generally higher 95th percentile mole fractions during winter months, however this pattern is not as clear as it is with NO and CO. The presence of near-field urban sources likely mask the natural seasonal variability in CH_4 mole fraction.

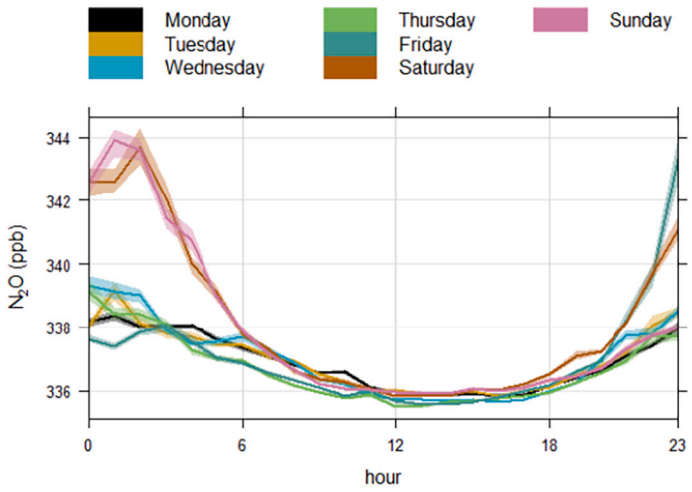

Fig. 8. Mean N_2O mole fraction variability with hour of the day. Solid lines represent mean values and shaded areas represent 95% confidence intervals.

3.3. Airmass and wind climatology

As shown in Fig. 9, the dominant wind directions over the course of the year-long measurement period are south westerly and east-south easterly. The strong and dominant southwesterly wind component is typical of prevailing westerly winds from the Atlantic in the north west of England. A marked east-southeasterly wind component is expected to be partially a result of the less obtrusive topography in the vicinity of the site. Buildings and trees in the area to the southeast of the site are relatively sparse compared with other radial directions. The presence of such obstacles may affect our ability to accurately and quantitatively capture the mean near-surface flow representative of the wider area around the measurement site. However, in this study, we only interpret measured wind direction in a broad and qualitiative sense to infer the likely upwind origins of sources of pollution observed at the MAQS site.

3.4. Spatial variability

Using measurements of wind direction and wind speed from the MAQS coincident with pollutant measurements, the spatial variability of enhancements and hence potential emission sources can be investigated. Fig. 10 shows polar annulus plots of selected trace gases from MAQS measurements, these plots show the variability of mean mole fraction with wind vector as well as showing temporal variability of mean mole fraction throughout the outer radius of the annulus (with the radial dimension representing hour-of-day). Fig. 10 therefore allows for spatial analysis of emission sources with temporal sensitivity (i.e. emissions from commuter traffic).

All species show moderately enhanced mole fractions from all wind directions, highlighting the dense urban location of the measurement site with emission sources distributed in all directions. However, there is a clear trend of high mean mole fractions hotspots to the northeast and southeast seen with all species in Fig. 10. The mean mole fraction hotspot to the northeast seen in all species could result from pollution from Manchester City Centre advected southwards towards the MAQS. The southeast mole fraction hotspot is likely a result of the complex urban topography within the study area as seen in Fig. 1, there are relatively few buildings situated to the southeast of the MAQS, therefore it is likely that airflow and hence pollution, is funnelled from the southeast due to the lack of building obstruction, this is also illustrated by the higher proportion of southeasterly wind directions shown in Fig. 9.

N_2O mole fraction does appear to show the same northeast and southeast hotspot activity as the other species, yet the largest mean N_2O mole fraction hotspot in excess of 342 ppb originates from a southwest wind direction. No emission hotspots from any of the other species in Fig. 10 are present from this wind vector, therefore suggesting that the majority of emissions from the previously identified recreational N_2O source may originate from the region west of the measurement site. It is worth noting that CH_4 mole fraction also exhibits a small mole fraction hotspot from the southwest wind direction, albeit not as prominent as with N_2O. This could potentially be a result of CH_4 emission from domestic gas heating systems (Lebel et al., 2020) and from natural gas distribution infrastructure supplying residential areas (McKain et al., 2015). Recreational N_2O use likely occurs from within residential buildings, so recreational N_2O emissions from the southwest could be coincident with CH_4 emissions from gas-powered heating systems in homes as well as gas leaks from pipelines supplying areas of housing.

The previous trend of nocturnal N_2O enhancements with a particular sensitivity for weekend nights is illustrated again in Fig. 11,

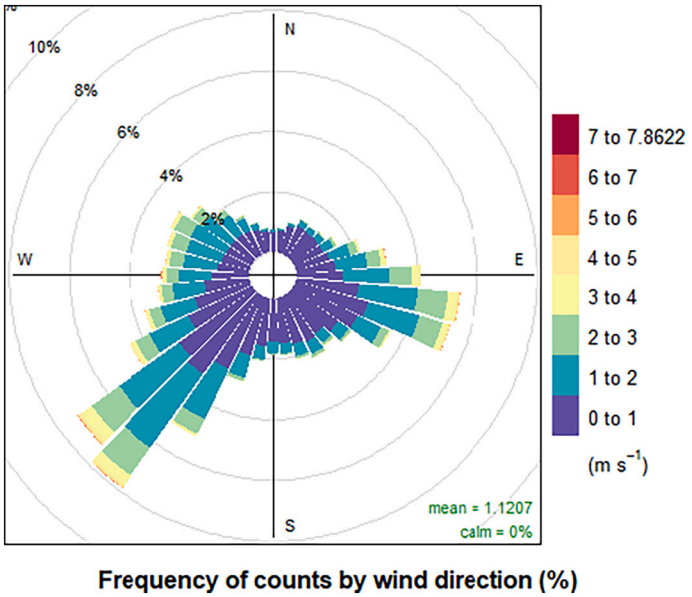

Fig. 9. Wind rose for measurements at the MAQS between October 2020 and October 2021, showing the percentage contribution of specific wind directions to all wind direction measurements. Wind rose segments are coloured by wind speed in m s^{-1}. (For interpretation of the references to colour in this figure legend, the reader is referred to the web version of this article.)

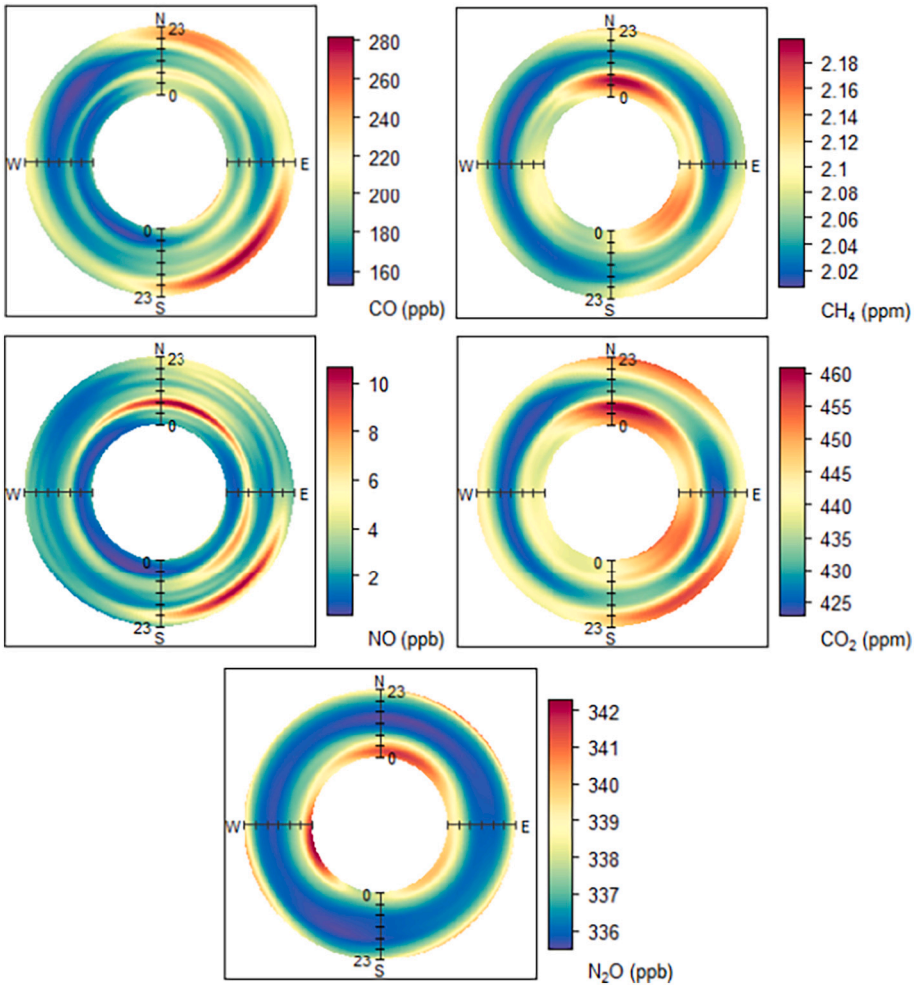

Fig. 10. Polar annulus plots of mean CH_4, CO_2, N_2O, NO, CO, and $PM_{2.5}$ concentration for October 2020 – October 2021 measurements at the MAQS.

with significantly higher mean N_2O mole fractions during the night as opposed to the day, and peak mean mole fractions in excess of 410 ppb occurring during Saturday night time. The nocturnal N_2O hotspots appear to orignate from a southwesterly direction in Fig. 11, reiterating the hotspot shown in the polar annulus plots of Fig. 8. Peak mean enhancements also appear to occur at relatively low wind speeds (< 2 m s^{-1}), which is consistent with a source relatively close to the site. As seen in Fig. 2, a number of student accomodation buildings are located to the immediate west of the measurement site which may contribute to this N_2O hotspot. Use of N_2O canisters at house parties both inside and outside university accomodation buildings may represent a nearby source location. As the measurement period coincided with COVID-19 lockdown restrictions, the frequency of the aforementioned house party events may have been higher relative to times without restricted social mobility, hence there is a reasonable likelihood that these areas of university accomodation may contribute to the nearby recreational N_2O source. However, other areas of student accomodation exist to the northeast of the site, which are not seen on the nocturnal polar plots in Fig. 11. In addition to student accomodation, a high-density area of terraced housing exists to the west of the measurement site past the student accomodation buildings it is possible that recreational use of N_2O from these residences could also contribute to the strong southwesterly nocturnal N_2O hotspot.

4. Conclusions and future work

In situ ground-based measurements of N_2O, alongside CH_4, CO_2, CO, NO_x, $PM_{2.5}$, and PM_{10} were made at the Manchester Air Quality Supersite situated in Fallowfield, Manchester between October 2020 and October 2021. Emissions of N_2O were detected that appeared to be independent of any other measured tracers. These N_2O emissions peaked at 02:00, and are independent from commuter traffic emissions seen in NO and CO. The diurnal pattern of N_2O enhancement was more prominent between the period of Friday night to Saturday morning than during weekday periods. The spatial origin of these emissions appears to be different to that of all other species measured at the supersite, with a peak mean N_2O mole fraction hotspot southwest of the measurement site, downwind of areas

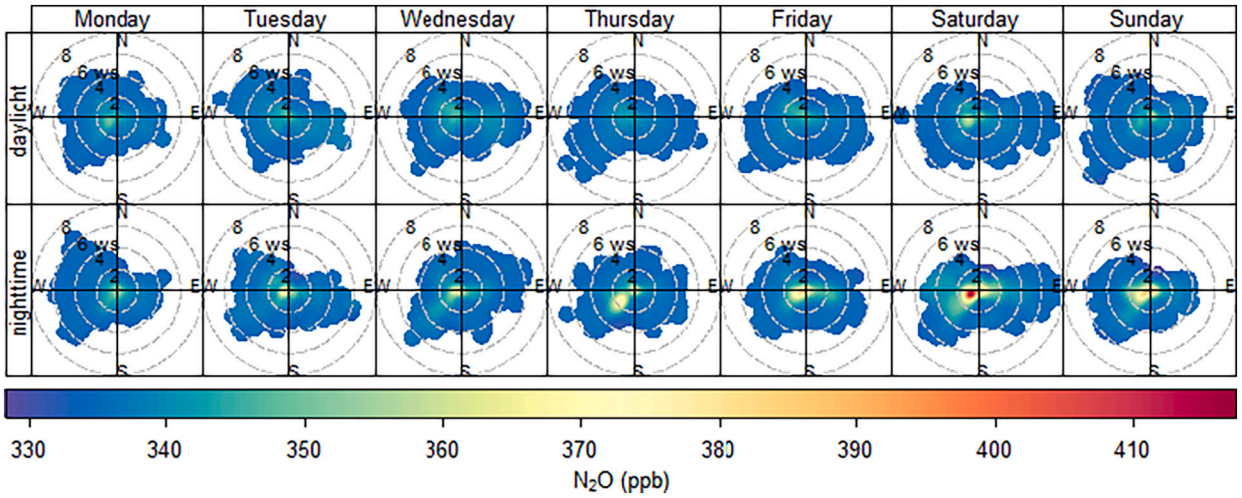

Fig. 11. Bivariate polar plots of mean N_2O mole fraction from the year-long measurement period. These plots show mole fraction variability with both wind direction and wind speed. The plots are divided into day of the week, and are also show measurements during daylight and nighttime hours.

of student accommodation and dense terraced housing. Both the temporal and spatial distribution of N_2O enhancement strongly suggest a significant nearby recreational source of N_2O from the use of N_2O whipped-cream chargers as a party drug. There has been very little previous study of N_2O emissions from its use as a recreational substance, and while the work here is purely qualitative, there is potential for this source to be significant due to the dominant temporal pattern in N_2O over more expected source patterns such as from commuter traffic. Future study should focus on quantification of this source, and comparison to NAEI for recreational N_2O.

Author contributions

P. A. Barker was the lead author, with writing contributions from G. Allen and S. Riddick. Data curation and validation was undertaken by P. A. Barker and M. Flynn. Formal data analysis was carried out by P. A. Barker. All co-authors provided commentary on draft versions of the manuscript.

Declaration of Competing Interest

The authors declare no conflict of interest.

Acknowledgements

The photograph used in Fig. 1 is licensed under CC BY 2.0. The basemap used in Fig. 2 is obtained from ArcGIS software (Sources: Esri, HERE,Garmin, Intermap, Increment P Corp., GEBCO, USGS, FAO, NPS, NRCAN, GeoBase, IGN, Kadaster NL, Ordnance Survey, Esri Japan, METI, Esri China (Hong Kong). © OpenStreetMap contributors and the GIS User Community). Figs. 6 – 10 were created using the Openair package in R (Carslaw and Ropkins, 2012). P. A. Barker is in receipt of a PhD studentship as part of the NERC Earth, Atmosphere and Ocean Doctoral Training Partnership (EAO DTP) (NERC grant reference no. NE/L002469/1).

References

Andreae, M., 2019. Emission of trace gases and aerosols from biomass burning—An updated assessment. Atmos. Chem. Phys. 1–27, 2019. https://doi.org/10.5194/acp-2019-303.

Banks, A., Hardman, J.G., 2005. Nitrous oxide. Contin. Educ. Anaesth. Crit. Care Pain 5 (5), 145–148. https://doi.org/10.1093/bjaceaccp/mki039.

Carslaw, D.C., Ropkins, K., 2012. *openair* - An r package for air quality data analysis. Environ. Model. Softw. 27–28, 52–61. https://doi.org/10.1016/j.envsoft.2011.09.008.

Daelman, M.R.J., van Voorthuizen, E.M., van Dongen, U.G.J.M., Volcke, E.I.P., van Loosdrecht, M.C.M., 2012. Methane emission during municipal wastewater treatment. Water Res. 46 (11), 3657–3670. https://doi.org/10.1016/j.watres.2012.04.024.

Davies, F., Middleton, D.R., Bozier, K.E., 2007. Urban air pollution modelling and measurements of boundary layer height. Atmos. Environ. 41 (19), 4040–4049. https://doi.org/10.1016/j.atmosenv.2007.01.015.

De Mello, W.Z., Ribeiro, R.P., Brotto, A.C., Kligerman, D.C., Piccoli, De S., Oliveira, J.L.M., 2013. Nitrous oxide emissions from an intermittent aeration activated sludge system of an urban wastewater treatment plant. Quim Nova 36 (1), 16–20. https://doi.org/10.1590/S0100-40422013000100004.

Ehirim, E.M., Naughton, D.P., Petróczi, A., 2018. No laughing matter: presence, consumption trends, drug awareness, and perceptions of "hippy crack" (nitrous oxide) among young adults in England. Front. Psychiatry 8 (JAN), 1–10. https://doi.org/10.3389/fpsyt.2017.00312.

Famulari, D., Nemitz, E., Di Marco, C., Phillips, G.J., Thomas, R., House, E., Fowler, D., 2010. Eddy-covariance measurements of nitrous oxide fluxes above a city. Agric. For. Meteorol. 150 (6), 786–793. https://doi.org/10.1016/j.agrformet.2009.08.003.

Helfter, C., Tremper, A.H., Halios, C.H., Kotthaus, S., Bjorkegren, A., Grimmond, C.S.B., Barlow, J.F, Nemitz, E., 2016. Spatial and temporal variability of urban fluxes of methane, carbon monoxide and carbon dioxide above London, UK. Atmos. Chem. Phys. 16, 10543–10557. https://doi.org/10.5194/acp-16-10543-2016.

IPCC, 2013. In: Stocker, T., Qin, D., Plattner, G.-K., Tignor, M., Allen, S., Boschung, J., Nauels, A., Xia, Y., Bex, V., Midgley, P. (Eds.), Anthropogenic and Natural Radiative Forcing, in: Climate Change 2013: The Physical Science Basis. Contribution of Working Group I to the Fifth Assessment Report of the Intergovernmental Panel on Climate Change. Cambridge University Press, Cambridge, United Kingdom and New York, NY, USA.

Järvi, L., Nordbo, A., Rannik, Ü., Haapanala, S., Mammarella, I., Pihlatie, M., Vesala, T., Riikonen, A., 2014. Urban nitrous-oxide fluxes measured using the eddy-covariance technique in Helsinki, Finland. Boreal Environ. Res. 19 (September), 108–121.

Kenagy, H.S., Sparks, T.L., Ebben, C.J., Wooldrige, P.J., Lopez-Hilfiker, F.D., Lee, B.H., Thornton, J.A., McDuffie, E.E., Fibiger, D.L., Brown, S.S., et al., 2018. NOx lifetime and NOy partitioning during WINTER. J. Geophys. Res. Atmos. 123 (17), 9813–9827. https://doi.org/10.1029/2018JD028736.

Ketzel, M., Wåhlin, P., Berkowicz, R., Palmgren, F., 2003. Particle and trace gas emission factors under urban driving conditions in Copenhagen based on street and roof-level observations. Atmos. Environ. 37 (20), 2735–2749. https://doi.org/10.1016/S1352-2310(03)00245-0.

Larin, I.K., Kuskov, M.L., 2014. Daytime and nighttime lifetimes of minor atmospheric components in the troposphere. Russ. J. Phys. Chem. B 8 (2), 254–260. https://doi.org/10.1134/S199079311402016X.

Lebel, E.D., Lu, H.S., Speizer, S.A., Finnegan, C.J., Jackson, R.B., 2020. Quantifying methane emissions from natural gas water heaters. Environ. Sci. Technol. 54 (9), 5737–5745. https://doi.org/10.1021/acs.est.9b07189.

McKain, K., Down, A., Raciti, S.M., Budney, J., Hutyra, L.R., Floerchinger, C., Herndon, S.C., Nehrkorn, T., Zahniser, M.S., Jackson, R.B., Phillips, N., Wofsy, S.C., 2015. Methane emissions from natural gas infrastructure and use in the urban region of Boston, Massachusetts. Proc. Natl. Acad. Sci. U. S. A. 112 (7), 1941–1946. https://doi.org/10.1073/pnas.1416261112.

NAEI/BEIS, 2022. National Atmospheric Emissions Inventory UK Emissions Data Selector [online] Available from: https://naei.beis.gov.uk/data/data-selector. Accessed 05 January 2022.

NOAA/GML, 2021. http://gml.noaa.gov/ccgg/trends_n2o (Accessed 12 November 2021).

Pitt, J.R., Le Breton, M., Allen, G., Percival, C.J., Gallagher, M.W., Bauguitte, J.-B., O'Shea, S.J., Muller, J.B.A., Zahniser, M.S., Pyle, J., Palmer, P.I., 2016. The development and evaluation of airborne in situ N2O and CH4 sampling using a quantum cascade laser absorption spectrometer (QCLAS). Atmos. Meas. Tech. 9 (1), 63–77. https://doi.org/10.5194/amt-9-63-2016.

Prather, M.J., Hsu, J., Deluca, N.M., Jackman, C.H., Oman, L.D., Douglass, A.R., Fleming, E.L., Strahan, S.E., Steenrod, S.D., Søvde, O.A., Isaksen, I.S.A., Froidevaux, L., Funke, B., 2015. Measuring and modeling the lifetime of nitrous oxide including its variability. J. Geophys. Res. Atmos. 120, 5693–5705. https://doi.org/10.1002/2015JD023267.

Randhawa, G., Bodenham, A., 2016. The increasing recreational use of nitrous oxide: history revisited. Br. J. Anaesth. 116 (3), 321–324. https://doi.org/10.1093/bja/aev297.

Ravishankara, A.R., Daniel, J.S., Portmann, R.W., 2009. Nitrous oxide (N_2O): The dominant ozone-depleting substance emitted in the 21st century. Science (80-.) 326 (5949), 123–125. https://doi.org/10.1126/science.1176985.

Squires, F.A., Nemitz, E., Langford, B., Wild, O., Drysdale, W.S., Joe, W., Fu, P., Sue, C., Hamilton, J.F., Nicholas Hewitt, C., Hollaway, M., Kotthaus, S., Lee, J., Metzger, S., Pingintha-Durden, N., Shaw, M., Vaughan, A.R., Wang, X., Wu, R., Zhang, Q., Zhang, Y., 2020. Measurements of traffic-dominated pollutant emissions in a Chinese megacity. Atmos. Chem. Phys. 20 (14), 8737–8761. https://doi.org/10.5194/acp-20-8737-2020.

Tallec, G., Garnier, J., Billen, G., Gousailles, M., 2008. Nitrous oxide emissions from denitrifying activated sludge of urban wastewater treatment plants, under anoxia and low oxygenation. Bioresour. Technol. 99 (7), 2200–2209. https://doi.org/10.1016/j.biortech.2007.05.025.

Tian, H., Xu, R., Canadell, J.G., Thompson, R.L., Winiwarter, W., Suntharalingam, P., Davidson, E.A., Ciais, P., Jackson, R.B., Janssens-Maenhout, G., Prather, M.J., et al., 2020. A comprehensive quantification of global nitrous oxide sources and sinks. Nature 586 (7828), 248–256. https://doi.org/10.1038/s41586-020-2780-0.

Townsend-Small, A., Czimczik, C.I., 2010. Carbon sequestration and greenhouse gas emissions in urban turf. Geophys. Res. Lett. 37, 1–5. https://doi.org/10.1029/2009GL041675.

UK Home Office, 2018. Drug Misuse: Findings from the 2017/18 Crime Survey for England and Wales [online] Available from. https://assets.publishing.service.gov.uk/government/uploads/system/uploads/attachment_data/file/729249/drug-misuse-2018-hosb1418.pdf. Accessed 22 June 2020.

van Amsterdam, J., Nabben, T., van den Brink, W., 2015. Recreational nitrous oxide use: prevalence and risks. Regul. Toxicol. Pharmacol. 73 (3), 790–796. https://doi.org/10.1016/j.yrtph.2015.10.017.

Van Delden, L., Rowlings, D.W., Scheer, C., Grace, P.R., 2016. Urbanisation-related land use change from forest and pasture into turf grass modifies soil nitrogen cycling and increases N2O emissions. Biogeosciences (II), 6095–6106. https://doi.org/10.5194/bg-13-6095-2016.

Vecchi, R., Bernardoni, V., Cricchio, D., D'Alessandro, A., Fermo, P., Lucarelli, F., Nava, S., Piazzalunga, A., Valli, G., 2008. The impact of fireworks on airborne particles. Atmos. Environ. 42 (6), 1121–1132. https://doi.org/10.1016/j.atmosenv.2007.10.047.

Yu, Z., Deng, H., Wang, D., Ye, M., Tan, Y., Li, Y., Chen, Z., Xu, S., 2013. Nitrous oxide emissions in the Shanghai river network: implications for the effects of urban sewage and IPCC methodology. Glob. Chang. Biol. 19 (10), 2999–3010. https://doi.org/10.1111/gcb.12290.

Zuck, D., Ellis, P., Dronsfield, A., 2012. Nitrous Oxide: Are You Having a Laugh? [online] Available from: http://www.rsc.org/eic. Accessed 11 June 2021.